Breaking the 11 kWh/kg Al barrier

M. Dupuis, GeniSim

It is important when performing a design study to establish a design goal. For the study presented here, the design goal was to break the 11 kWh/kg$_{Al}$ cell energy consumption barrier, because this was judged to be an achievable short-term design goal.
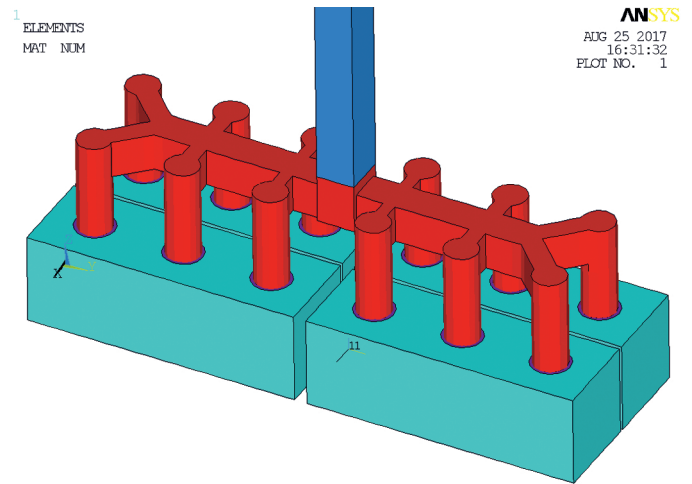
Introduction

The R&D design work presented in this article is the immediate follow-up of what was presented by the author presented in a paper at the 2018 TMS conference [1]. In that paper he studied two designs. The first one is based on a cathode design where 100% of the cell current is extracted from its downstream side [2, 3]. In [1], the outcome of the study is a 500 kA, 100% downstream current extraction cell design, operating in thermal balance at 11.2 kWh/kg$_{Al}$. Yet the future work section proposed some ideas to further reduce the cell energy consumption. The present study implemented those ideas.

In [1], the second design is based on using a wider cell, an idea initially presented a year ago in this Journal [4]. That wider cell uses the Reversed Compensation Current (RCC) busbar concept first shown in [5]. The outcome of the study is a 650 kA, wider cell design operating in thermal balance at 11.3 kWh/kg$_{Al}$. Again in [1], the future work section proposed some ideas to further reduce the cell energy consumption and the present study tested those ideas as well.
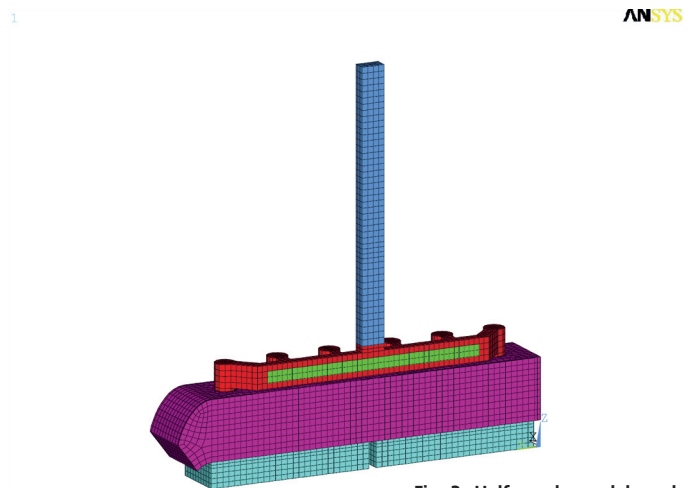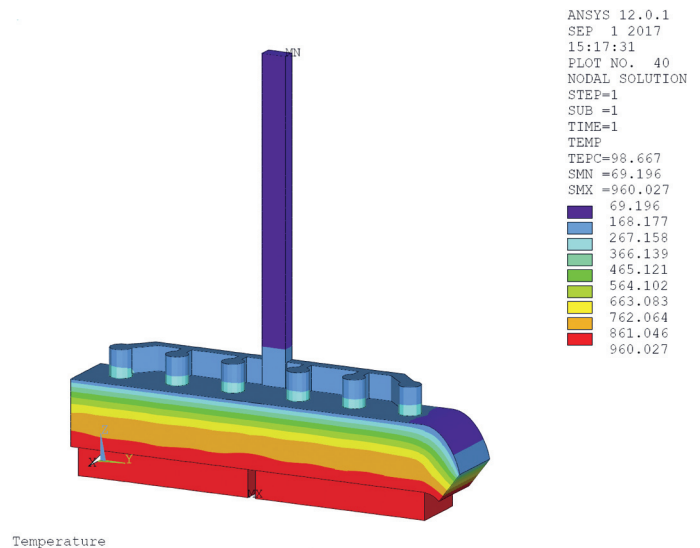

Half anode: 650 kA anode model

Fig. 1: Topology of the 4 carbon blocks per anode, 3 stubs per carbon block new anode design

Half anode: 650 kA anode model

Fig. 2: Half anode model mesh showing the copper insert in green

Table 1: Design 1, Wider 650 kA cell using RCC busbar design

Amperage	762.5 kA	650 kA	650 kA
Nb. of anodes	48	48	36
Anode size	2.6 x .65 m	2.6 x .65 m	2.6 x .86 m
Nb. of anode studs	4 per anode	4 per anode	12 per anode
Anode stud diameter	21.0 cm	24.0 cm	16.0 cm
Anode cover thickness	15 cm	24 cm	25 cm
Nb. of cathode blocks	24	24	24
Cathode block length	5.37 m	5.37 m	5.37 m
Type of cathode block	HC 10	HC 10	HC 10
Collector bar size	20 x 12 cm	20 x 15 cm	20 x 15 cm
Type of side block	HC3	HC3	HC3
Side block thickness	7 cm	7 cm	7 cm
ASD	25 cm	25 cm	25 cm
Calcium silicate thickness	3.5 cm	6.0 cm	6.0 cm
Inside potshell size	17.02 x 5.88m	17.02 x 5.88m	17.02 x 5.88m
ACD	3.0 cm	2.8 cm	2.8 cm
Excess AlF$_3$	11.50%	11.50%	11.50%
Anode drop (A)	347 mV	296 mV	252 mV
Cathode drop (A)	118 mV	109 mV	109 mV
Busbar drop (A)	300 mV	220 mV	170 mV
Anode panel heat loss (A)	553 kW	327 kW	339 kW
Cathode total lieat loss (A)	715 kW	499 kW	482 kW
Operating temperatur (D/M)	968.9 °C	967.0 °C	966.5 °C
Liquidus superheat (D/M)	10.0 °C	8.1 °C	7.6 °C
Bath ledge thickness (A)	6.82 cm	11.86 cm	14.25 cm
Metal ledge thickness (A)	1.85 cm	3.38 cm	4.58 cm
Current efficiency (D/M)	95.14%	94.80%	94.90%
Intenial heat (D/M)	1328 kW	832 kW	804 kW
Energy consumption	12.85 kWh/kg	11.3 kWh/kg	11.0 kWh/kg

Temperature

Fig. 3: Anode model temperature solution

Design 1: Wider 650 kA cell using RCC busbar design

In [1], it was concluded that the 2 carbon blocks per anode, 2 stubs per carbon block anode design was limiting the possibilities to further reduce the anode voltage drop. For that reason, the current study developed a new anode model in order to test a new 4 carbon blocks per anode, 3 stubs per carbon block anode design. Fig. 1 presents the new anode model topology. This keeps the anode block surface
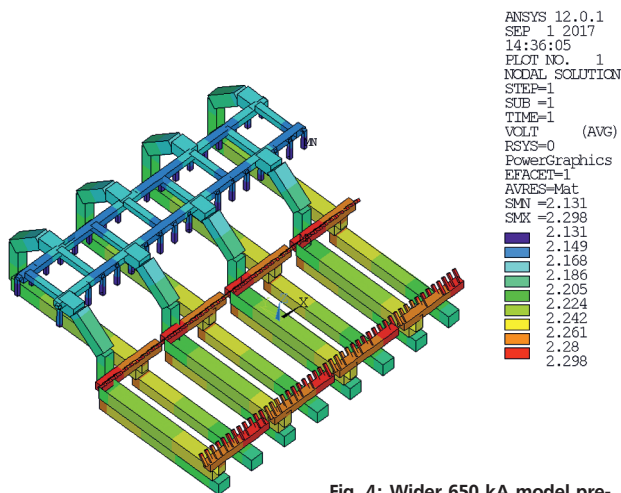

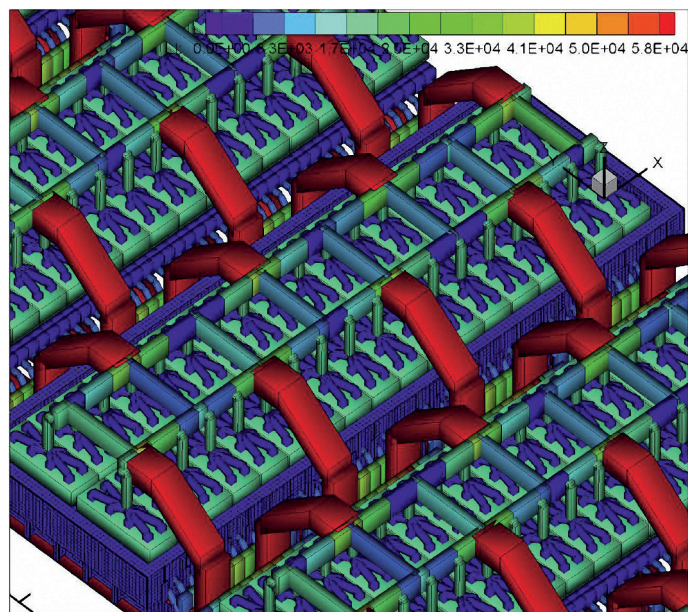Fig. 4: Wider 650 kA model predicted busbar voltage drop

Fig. 5: Wider 650 kA 8 risers RCC busbar network MHD-Valdis model setup
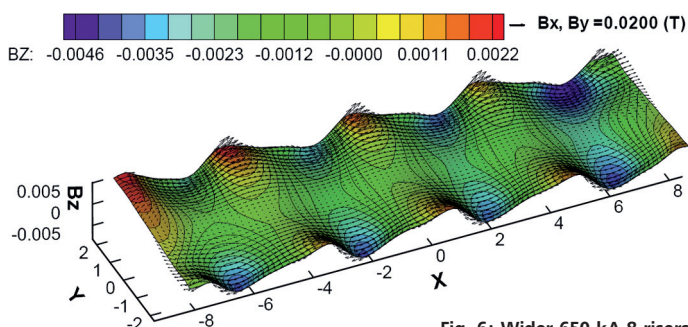

Fig. 6: Wider 650 kA 8 risers RCC busbar network MHD-Valdis model BZ prediction

horizontal in order to simplify the model topology. A more detailed model will include extra features to minimize the carbon usage. As Table 1 indicates, the global anode length has remained unchanged with 4 carbon blocks of 1.3 x 0.43 metres for a total area of 2.6 x 0.86 metres per anode. Since there are 3 stubs per carbon blocks, each stub is providing current to an almost square 0.433 x 0.43 metres carbon surface area. The new stub diameter is 16 cm.

As in the initial concept presented in [4], there is a 6 cm wide channel between the front and back carbon blocks to enhance electrolyte flow and mixing. There is a smaller 2 cm channel between the 2 side-by-side carbon blocks, and there is room for 36 such anodes in that wider cell. As Fig. 1 indicates, the new anode design is characterized by a very long horizontal yoke. As Fig. 2 indicates, a copper insert inserted in that yoke further reduces the anode electrical resistance, and hence the anode voltage drop, without increasing the anode heat loss. Fig. 3 shows the obtained temperature solution. As Table 1 indicated, the anode cover is 25 cm thick, which is a lot, but it insulates to reduce the anode heat loss. The anode hole design incorporates the patented idea to pass current in the horizontal contact between the stud and the carbon [6]. The anode also incorporates a non-described design feature that further reduces the anode heat loss. As Table 1 indicates, the predicted anode voltage drop is 252 mV, a 44 mV reduction over the predicted 296 mV anode drop reported for the anode design presented in [1]. The predicted anode panel heat loss is 339 kW, 12 kW more than the 327 kW predicted for the anode design presented in [1].

In [1], it was also recommended to further optimized the RCC busbar network in order to reduce even more the reported 220 mV busbar drop. As presented in Fig. 5 of [1], that RCC busbar network is using a total of 6 risers, 3 on the upstream side and 3 more offset on the downstream side. That network of 6 RCC busbars was replaced by a network of 8 risers RCC busbars, with 4 risers on the upstream side and 4 more offset on the downstream side, as presented in Fig. 4. As Table 1 shows, this much lowers the busbar voltage drop, predicted down by 50 mV to 170 mV.

Fig. 5 presents the global setup of the MHD model. Notice that MHD-Valdis does not support a 4 blocks per anode, 3 stubs per block anode design, so a single block 8 stubs anode design was selected instead. Figs 6-8 present respectively the obtained B_Z, bath-metal interface deformation and metal flow field. As the MHD results indicate, the 8 risers RCC busbar design is even better than the 6 risers RCC busbar design. As Table 1 finally shows, after the change of both the anode and the busbar, the third version (right column of Table 1) of the wider cell, still operating at 650 kA, is predicted to operate in thermal balance, dissipating only 804 kW. It consumes exactly 11.0 kWh/kg_{Al}, which is reaching but not breaking the 11.0 kWh/kg_{Al} barrier!

Design 2: 520 kA cell with 100% downstream side current extraction

The reduction of the cell energy consumption is always a compromise to balance the cell's lower internal heat generation (hence lower ohmic resistance components of the cell voltage) against the reduction of the cell heat loss. The dilemma comes from the fact that reducing the electrical resistance of cathode and the anode will also typically reduce the thermal resistance of those ohmic components. This means that limits to further reduction of the cell energy consumption exists both on the heat production side and on the heat dissipation side. For Design 1, the limitation is on the heat production side, as a

wider cell dissipates less heat per unit production. But on the other hand this makes it more difficult to lower the electrical resistance of the ohmic components like the busbar.

Design 2 shows the opposite situation: lowering the ACD from 3.2 to 2.8 cm automatically reduces the cell internal heat generation, but at 500 kA, it was not possible to find a way to operate the cell in thermal balance at a 'reasonable' cell superheat. So the cell amperage had to be increased to 520 kA in order to maintain the cell internal heat around 700 kW, as indicated in Table 2. Of course, this change of ACD and amperage means that the anode and cathode models must be rerun to analyze the impact of those two operational changes. These new results are also reported in Table 2 third column: first the anode drop increases by 10 mV from 238 to 248 mV, without significant change to the anode panel heat loss. Second, the cathode voltage drop increases by 3 mV from 125 to 128 mV, again without significant impact on the cathode heat loss, bit at the expense of a slight reduction of the cell superheat from 5.4 to 5.3 °C. Some people would argue that it is not possible to operate a cell at such a low cell superheat, yet the author remembers having deliberately designed the cell lining of the A310 cell so that it would operate a 6 °C of cell liquidus superheat. This cell operated quite well at that predicted superheat and predicted ledge thickness, although with a much greater bath volume than was usual at that time.

The second recommendation for this '500' kA cell with 100% downstream side current extraction was shrink the cell centre-to-centre distance from 7 metres in the previous design, reported in [1]. That distance has been reduced to 6.2 metres in the current study. It was easy to significantly reduce that distance, because that important

cell design parameter has not previously been optimized. At the same time, the thicker busbar sections further reduce the busbar voltage drop, which was already quite low due to the 100% downstream side current extraction consisting only of anode risers. The number was kept to 6 risers, but on second thoughts, again it might have been
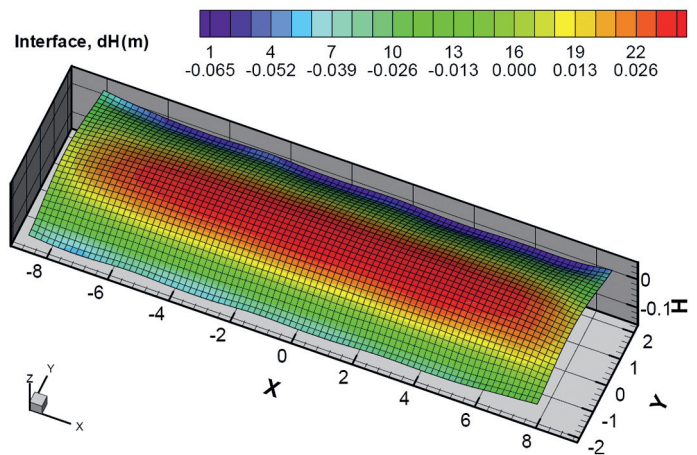

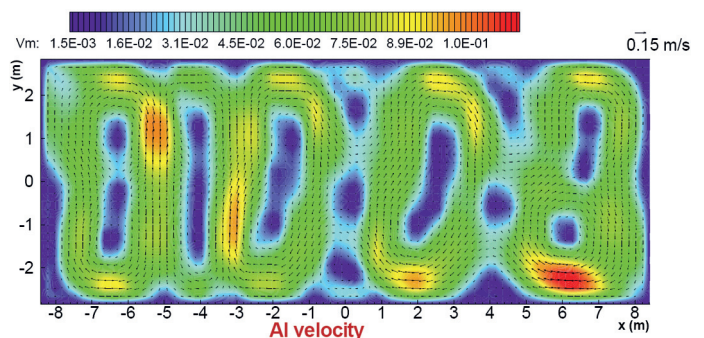**Fig. 7: Wider 650 kA 8 risers RCC busbar network MHD-Valdis model bath-metal interface prediction**

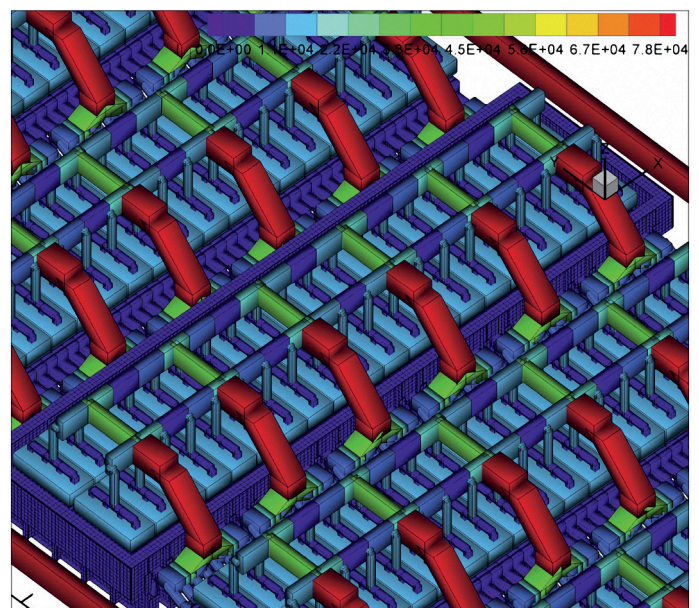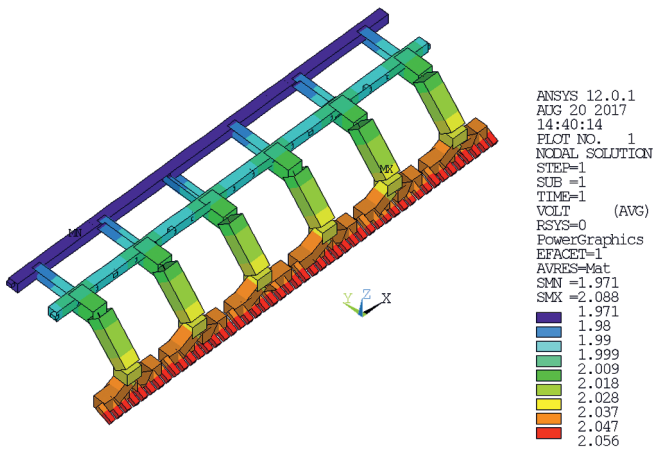**Fig. 8: Wider 650 kA 8 risers RCC busbar network MHD-Valdis model metal flow field prediction**

Fig. 9: 520 kA 6 risers 100% downstream current extraction cell with ECC busbar network, MHD-Valdis model setup

Table 2: Design 2, 520 kA cell with 100% downstream side current extraction

	600 kA	500 kA	520 kA
Amperage	600 kA	500 kA	520 kA
Nb. of anodes	48	64	64
Anode size	2.0 x .665 m	1.95 x .5 m	1.95 x .5 m
Nb. of anode studs	4 per anode	4 per anode	4 per anode
Anode stud diameter	17.5 cm	17.5 cm	17.5 cm
Anode cover thickness	10 cm	20 cm	20 cm
Nb. of cathode blocks	24	24	24
Cathode block length	4.17 m	4.17 m	4.17 m
Type of cathode block	HC 10	HC 10	HC 10
Collector bar size	20 x 10 cm	20 x 20 cm	20 x 20 cm
Type of side block	SiC	HC3	HC3
Side block thickness	7 cm	7 cm	7 cm
ASD	28 cm	30 cm	30 cm
Calcium silicate thickness	3.5 cm	6.0 cm	6.0 cm
Inside potshell size	17.8 x 4.85 m	17.8 x 4.85 m	17.8 x 4.85 m
ACD	3.5 cm	3.2 cm	2.8 cm
Excess AlF$_3$	12%	12%	12%
Anode drop (A)	318 mV	238 mV	248 mV
Cathode drop (A)	104 mV	123 mV	182 mV
Busbar drop (A)	311 mV	134 mV	85 mV
Anode panel heat loss (A)	449 kW	292 kW	295 kW
Cathode total lieat loss (A)	692 kW	402 kW	404 kW
Operating temperatur (D/M)	964.8 °C	958.4 °C	958.3 °C
Liquidus superheat (D/M)	11.8 °C	5.4 °C	5.3 °C
Bath ledge thickness (A)	6.36 cm	11.84 cm	11.83 cm
Metal ledge thickness (A)	1.76 cm	3.48 cm	3.46 cm
Current efficiency (D/M)	96.4%	96.3%	96.5%
Intenial heat (D/M)	1140 kW	699 kW	701 kW
Energy consumption	13.26 kWh/kg	11.2 kWh/kg	10.85 kWh/kg

```
ANSYS 12.0.1
AUG 20 2017
14:40:14
PLOT NO.   1
NODAL SOLUTION
STEP=1
SUB =1
TIME=1
VOLT      (AVG)
RSYS=0
PowerGraphics
EFACET=1
AVRES=Mat
SMN =1.971
SMX =2.088
```

External Compensation Current

Fig. 10: 520 kA 6 risers 100% downstream current extraction cell with ECC busbar network predicted voltage drop

Fig. 11: 520 kA 6 risers 100% downstream current extraction cell with ECC busbar network predicted BZ
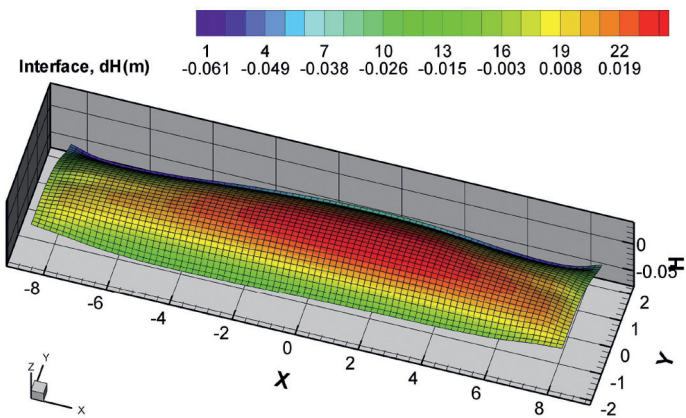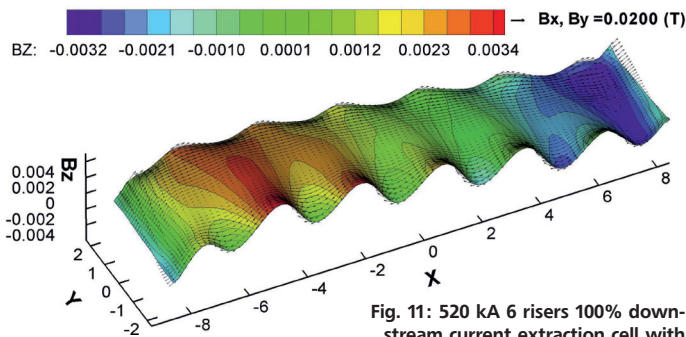

Fig. 12: 520 kA 6 risers 100% downstream current extraction cell with ECC busbar network: predicted bath-metal interface
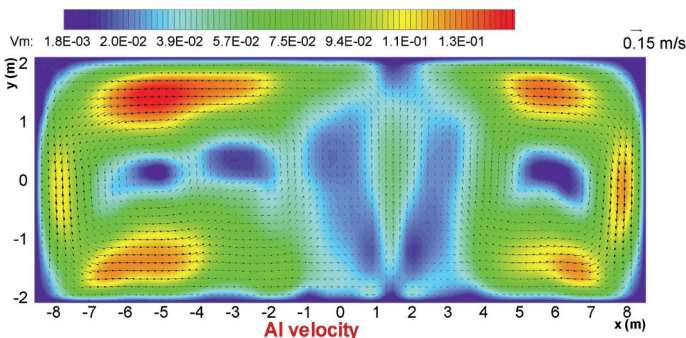

Fig. 13: 520 kA 6 risers 100% downstream current extraction cell with ECC busbar network: predicted metal flow field

better to increase that to 8 risers, as it is the cross section of the risers that prevented further shrinking of the cell pot-to-pot distance as shown in Fig. 9. Fig. 10 presents the obtained busbar voltage drop of 85 mV, a reduction of 49 mV over the 134 mV of the previous design, despite the increase of the cell amperage.

This drastic lowering of the busbar voltage drop obviously greatly contributes to lowering the cell power consumption. Another great advantage of reducing that component of the cell ohmic resistance is that it does not affect the cell heat balance. Figs 11-13 demonstrate that the cell MHD is not negatively affected by the shrinking of the pot-to-pot distance to 6.2 metres.

The present study achieves its design goal to break the 11.0 kWh/kg_{Al} barrier, as Table 2 proves. The new version of the 520 kA cell, with 100% downstream side current extraction, is predicted to consume only 10.85 kWh/kg_{Al} produced, well below the 11.0 mark.

Comparison of the two cell design options

The comparison exercise presented in [1] is repeated here, using the updated designs for both options. On the opex side, the discrepancy has increased to 0.15 kWh/kg_{Al}, now that the two cell designs are operated at the same 'minimum' 2.8 cm of ACD. Clearly the busbar length requirement is what most differentiates the two cell designs which both favour of the 100% downstream side current extraction cell design option.

On the capex side, a very crude comparison was made in [1]. Based on the length of potroom(s) required for a smelter to produce 1 million tonnes of aluminium per year, that number of cells has not changed for the wider cell design option: at 95% current efficiency, a 650 kA cell produces 4.974 tonnes Al per day. So it needs 550 cells, and with a 7.5 metres of pot-to-pot distance, requires 4.2 km of potroom(s) to host them. On the other hand, that number of cells has been improved for the 100% downstream current extraction cell design option. At 95% current efficiency, a 520 kA cell produces 3.980 tonnes Al per day, so it needs 688 cells and with a 6.2 metres of pot-to-pot distance, it requires 4.3 km of potrooms to host them. Clearly, increasing the cell amperage, and at the same time reducing the pot-to-pot distance, had a big impact on the capex of that cell design option. Yet it is important to remember the savings that the RCC busbar concept offers when it is used in the wider cell design option. RCC does not require a return line located 60 metres away, nor a set of independent rectifiers to power any external compensation busbar loops, as the EEC busbar concept needs for the 100% downstream side current extraction cell design.

Future work

It is the opinion of the author that further reduction of the cell energy consumption will probably have to come from recovering of some of the heat lost by the cell. At the recent ICSOBA conference in Hamburg, such a heat recovery system (HRS) was presented by EGA [7]. Fig. 14 from [7] presents the HRS concept, where heat can be extracted both from the cell exhaust gas and from the cell side walls. According to [7], 120 kW can on average be collected by the side wall heat exchangers. No data was provided in [7] for the conversion efficiency, but in their TMS 2014 paper [8], Goodtech Recovery Technology, that provided the HRS to EGA, was talking of only 10%, admittedly on the conservative side. Based on [9], it may be reasonable to assume 20% of conversion efficiency. On that basis, out of the 120 kW of cell heat loss collected, 24 kW can be converted
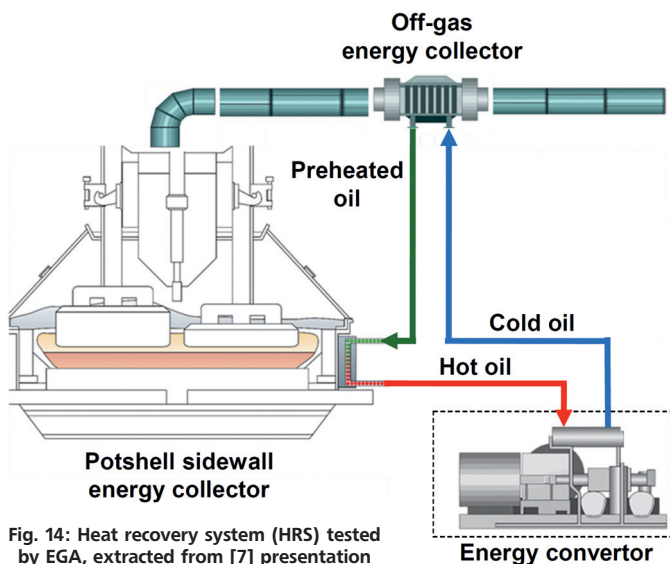
Fig. 14: Heat recovery system (HRS) tested by EGA, extracted from [7] presentation

back into electrical energy, which for a 455 kA cell represents 53 mV or 0.165 kWh/kg$_{Al}$.

On the cell exhaust gas heat recovery, it would be far more efficient to first increase the gas exhaust temperature. This could be achieved by reducing the area of the hood openings and also by insulating the hoods and the fume plate so as to decrease the gas exhaust flow rate and to keep more of the anode panel heat loss in the exhaust gas. Also at the ICSOBA conference, the author presented a model that was developed to study the impact of such design changes [10] on the cell hooding system heat balance and the cell hooding HF capture efficiency. If the equivalent amount of heat collected on the cell side walls can be collected from the gas exhaust and converted into electrical energy, we are talking about a potential of 100 mV or about 0.31 kWh/kg of cell energy consumption reduction due to HRS having only 20% conversion efficiency.

Discussion and conclusions

Contrary to the author's expectations one year ago, the present study has produced cell designs that have reached, and in the second case broken, the 11.0 kWh/kg$_{Al}$ cell energy consumption barrier. At 10.85 kWh/kg$_{Al}$, at the time of writing this paper, the author ran out of design idea to further reduce that number without involving HRS. Even with heat recovery, the very low conversion rate of such low grade heat energy into electrical energy means that HRS has the potential to further decrease the cell energy consumption by another 0.31 kWh/kg$_{Al}$, down to about 10.54 kWh/kg$_{Al}$. This is still 0.54 kWh/kg$_{Al}$ away from the next barrier to be broken, the 10.0

kWh/kg$_{Al}$ barrier.

Clearly, it would be far more efficient to use that captured, low grade heat energy to preheat the alumina and/or the anodes, or maybe use it to reduce the fuel consumption in the anode baking furnace. In such a case the 0.31 kWh/kg$_{Al}$ of cell energy consumption reduction becomes 1.55 kWh/kg$_{Al}$, plenty to break the 10.0 kWh/kg$_{Al}$ barrier and even to start dreaming of breaking the next barrier!

References

[1] M. Dupuis, Very low energy consumption cell designs: the cell heat balance challenge, TMS Light Metals, 2018, to be published.

[2] M. Dupuis, A new aluminium electrolysis cell busbar network concept, Proceedings of 34th International ICSOBA Conference, Québec City, Canada, 3 – 6 Oct. 2016, Paper AL39, Travaux No. 45, 883-890.

[3] M. Dupuis, Low energy consumption cell design involving copper inserts and innovative busbar network layout, TMS Light Metals, 2017, 693-703.

[4] M. Dupuis and B. Welch, Designing cells for the future – wider and/or even higher amperage?, ALUMINIUM, 93 (1/2), 2017, 45-49.

[5] M. Dupuis, A new aluminium electrolysis cell busbar network concept, Proceedings of 33rd International ICSOBA Conference, Dubai, UAE, 29 Nov. – 1 Dec. 2015, Paper AL21, Travaux No. 44, 699-708.

[6] M. Dupuis, Presentation of a New Anode Stub Hole Design Reducing the Voltage Drop of the Connection by 50 mV, VIII International Congress & Exhibition Non-Ferrous Metals and Minerals, Krasnoyarsk, Russia, 13 – 16 Sept. 2016, https://drive.google.com/file/d/0Bwb-wQZ90LvBVF9WWQ0LWZZdTQ/view.

[7] A. AlJasmi and A. AlZarouni, Findings from operating a pot with heat recovery system, Proceedings of 35th International ICSOBA Conference, Hamburg, Germany, 2 – 5 Oct. 2017, Paper AL29, Travaux No. 46, 1071-1080.

[8] Y. M. Barzi, M. Assadi and H. M. Arvesen, A novel heat recovery technology from an aluminum reduction cell side walls: experimental and theoretical investigations, TMS Light Metals, 2014, 733-738.

[9] T. C. Hung, T. Y. Shai and S. K. Wang, A review of organic rankine cycles (ORCs) for the recovery of low-grade waste heat, Energy, 1997, Vol. 22(7), 661-667.

[10] M. Dupuis, M. Pagé and F. Julien, Development of an Autodesk CFD-Based 3D Model of a Hall Héroult Cell Hooding System and HF Capture Efficiency, Proceedings of 35th International ICSOBA Conference, Hamburg, Germany, 2 – 5 Oct. 2017, Paper AL07, Travaux No. 46, 835-850.

Author

Dr. Marc Dupuis is a consultant specialized in the applications of mathematical modelling for the aluminium industry since 1994, the year when he founded his own consulting company GeniSim Inc. (www.genisim.com). Before that, he graduated with a Ph.D. in chemical engineering from Laval University in Quebec City in 1984, and then worked ten years as a research engineer for Alcan International. His main research interests are the development of mathematical models of the Hall-Héroult cell, dealing with the thermo-electric, thermo-mechanical, electro-magnetic and hydrodynamic aspects of the problem. He was also involved in the design of experimental high amperage cells and in the retrofit of many existing cell technologies.